Research Square

Preprints are preliminary reports that have not undergone peer review.
They should not be considered conclusive, used to inform clinical practice,
or referenced by the media as validated information.

AmpR-free yeast display of six sexual-stage Eimeria tenella antigens as candidate oral vaccines against chicken coccidiosis

Jinwen Wang
Shanghai Veterinary Research Institute
Yan Cai
Southwest Minzu University
Zhen Feng
Animal, Plant and Food Inspection Center of Nanjing Customs District
Qiping Zhao
Shanghai Veterinary Research Institute
Shunhai Zhu
Shanghai Veterinary Research Institute
Yu Yu
Shanghai Veterinary Research Institute
Jiayu Bai
Shanghai Veterinary Research Institute
Wenqi Han
Shanghai Veterinary Research Institute
Shanbo Wu
Shanghai Veterinary Research Institute
Fanghe Zhao
Shanghai Veterinary Research Institute
Hongyu Han
Shanghai Veterinary Research Institute
Hui Dong
donghui@shvri.ac.cn

Shanghai Veterinary Research Institute

Research Article

Keywords: Coccidiosis, Eimeria tenella, Transmission-blocking vaccine, AmpR-free yeast display, Sexual-stage antigens, EtGFAT

Posted Date: November 23rd, 2026

DOI: https://doi.org/10.21203/rs.3.rs-11623007/v1

License: This work is licensed under a Creative Commons Attribution 4.0 International License.
Read Full License

Additional Declarations: No competing interests reported.

AmpR-free yeast display of six sexual-stage *Eimeria tenella* antigens as candidate oral vaccines against chicken coccidiosis

Jinwen Wang[a], Yan Cai[a,b], Zhen Feng[c], Qiping Zhao[a], Shunhai Zhu[a], Yu Yu[a], Jiayu Bai[a], Wenqi Han[a], Shanbo Wu[a], Fanghe Zhao[a], Hongyu Han[a*], Hui Dong[a*]

[a]Shanghai Veterinary Research Institute, Chinese Academy of Agricultural Sciences, Minhang, Shanghai, 200241, PR China

[b]College of Animal Husbandry and Veterinary Medicine, Southwest Minzu University, Chengdu, 610041, PR China

[c]Animal, Plant and Food Inspection Center of Nanjing Customs District, Nanjing 210001, PR China

[*]Corresponding authors.

Abstract

Background

Targeting the sexual stages of *Eimeria tenella* is critical for curtailing environmental transmission, yet effective recombinant strategies remain underdeveloped, and current expression systems generally rely on antibiotic-resistance markers that risk leaking into the gut ecosystem.

Results

To address these challenges, we engineered an *AmpR*-free, *TRP1*-complemented *Saccharomyces cerevisiae* platform for yeast surface display and evaluated six sexual-stage-upregulated *E. tenella* antigens (*Et*GFAT, *Et*Sub4, *Et*AKRO, *Et*GBE, *Et*4aGT, and *Et*α-AMY) as candidate oral vaccines. Strikingly, protective efficacy was decoupled from antigen surface-display efficiency. The *Et*GFAT vaccine induced the highest comprehensive protection

(ACI=143), reducing oocyst shedding by approximately 50% and mitigating cecal lesions. This robust defense was mechanistically supported by the strongest peripheral $CD3^+CD4^+$/$CD3^+CD8^+$ T-cell responses and a significant downregulation of local pro-inflammatory cytokines (IL-1β, IL-6, and IL-8) in the cecum. Furthermore, the splenic cytokine profiles revealed distinct systemic signatures: *Et*Sub4 preferentially drove a Th1-biased response, whereas *Et*GFAT significantly suppressed the Th2-associated cytokine IL-4 while maintaining IL-10 levels. Although *Et*GBE conferred partial protection (ACI=138), antigens linked to energy metabolism generally showed limited efficacy.

Conclusions

Our findings identify *Et*GFAT as a premier candidate for transmission-blocking vaccines and validate the *AmpR*-free yeast chassis as a safe, environmentally sustainable platform for rational oral vaccine design against chicken coccidiosis.

Keywords: Coccidiosis; *Eimeria tenella*; Transmission-blocking vaccine; AmpR-free yeast display; Sexual-stage antigens; *Et*GFAT

Background

Avian coccidiosis, caused by several *Eimeria* species including the highly pathogenic *Eimeria tenella*, remains one of the most economically important diseases of poultry worldwide [1,2]. *Eimeria* parasites have a direct faecal–oral life cycle, and transmission is driven by the shedding of environmentally resistant oocysts that contaminate litter and facilitate reinfection under intensive production systems [3]. Current control relies mainly on anticoccidial drugs and live-oocyst vaccines, but drug resistance, chemical residues, the high cost and logistical burden of live-vaccine production, and biosafety concerns have created an urgent need for alternative

vaccine strategies [2,4]. Among these alternatives, recombinant vaccines have been extensively pursued; however, most such vaccines developed so far still target invasion-related antigens, such as microneme and rhoptry proteins, which act at the sporozoite and merozoite stages to block host-cell entry [5,6]. Although such antigens can reduce parasite invasion and replication, their capacity to limit the sexual stages that produce oocysts—and therefore to reduce environmental contamination and onward transmission-has not been directly established and may be limited [4,7].

A conceptually different approach is transmission-blocking vaccination, which aims to interfere with parasite development at the sexual stages, reducing oocyst formation and shedding and thereby lowering environmental contamination and onward transmission [7]. Pioneering studies on *Eimeria* showed that maternal antibodies against gametocyte antigens could substantially reduce oocyst output in offspring chicks, and parallel studies on *Cryptosporidium and Plasmodium* supported the broader potential of transmission-blocking immunity [7,8]. In poultry, this concept was translated into CoxAbic®, a subunit vaccine based on affinity-purified antigens from the wall-forming bodies of *E. maxima* macrogametocytes, which has been field-tested in multiple countries and provides proof of principle that sexual-stage antigens can reduce *Eimeria* transmission [4,9]. However, CoxAbic® depends on native antigens purified from infected intestinal tissue, which is laborious and costly [4,10]; recombinant sexual-stage antigens could overcome this manufacturing limitation but require systematic identification of protective candidates. Transcriptomic profiling of *E. tenella* gametocytes has identified sexual-stage-upregulated genes, many of which encode proteins involved in oocyst wall biosynthesis and fertilization, thus providing a rational candidate pool for transmission-blocking

vaccines [11]. Consistent with this, recombinant gametocyte antigens such as *Et*Gam22 and *Et*GAM56 reduced oocyst output by 45-78% in experimental challenge studies [12,13]. Although these estimates vary with antigen, delivery system and challenge model, they support the potential of sexual-stage proteins for transmission-blocking immunity.

Saccharomyces cerevisiae is an attractive host for oral vaccine delivery because, as a eukaryotic microorganism, it can express eukaryotic antigens with post-translational modifications, is generally regarded as safe for food and feed applications, and its cell wall β-glucan, mannan and chitin can activate innate and adaptive immune responses [14,15]. Yeast surface display further anchors antigens on the cell surface and improves delivery to the gut-associated lymphoid tissues, where *Eimeria* completes its life cycle [16,17]. These features have supported the development of yeast-based oral vaccines displaying multiple *Eimeria* antigens, including invasion-related microneme and rhoptry proteins, which conferred varying degrees of protection in challenge studies [16–18]. The dendritic-cell-targeting peptide DCpep has also been explored as a means to improve antigen delivery and immune recognition in several recombinant oral vaccine systems [19–21], and may enhance the immunogenicity of yeast-displayed *Eimeria* antigens; however, its specific contribution in this setting remains to be directly demonstrated.

However, many of these previously displayed *Eimeria* antigens act at the invasion stage, and the corresponding yeast display platforms have generally retained conventional antibiotic-resistance markers. Whether the same system can be redirected toward sexual-stage antigens remains unresolved; moreover, plasmid-borne resistance markers raise concrete biosafety concerns because resistance genes can leak into the gut ecosystem and disseminate to commensal or pathogenic bacteria. Although *S. cerevisiae* is not known to naturally acquire or spread such

antibiotic-resistance genes, retaining a plasmid-borne marker undermines this intrinsic biosafety advantage, and current regulatory guidelines increasingly discourage resistance markers in orally administered vaccines for food-producing animals [22]. For sexual-stage antigens, an antibiotic-resistance-marker-free platform is therefore needed.

To address these gaps, we deleted the entire *AmpR* gene from the pYD1-antigen-DCpep constructs and transformed the resulting *AmpR*-free plasmids into *Saccharomyces cerevisiae* EBY100. Transformants were selected on SD-Trp medium through *TRP1* complementation, establishing an *AmpR*-free, *TRP1*-complemented yeast surface-display platform. Using this platform, we evaluated six sexual-stage-upregulated *Eimeria tenella* antigens (**Table 1**) as candidate transmission-blocking vaccine antigens, to determine whether these antigens can confer protection and whether functional annotation is associated with protective efficacy.

Results

Construction and confirmation of *AmpR*-free recombinant yeast strains

To establish an antibiotic-resistance-marker-free yeast surface-display platform, we first constructed the intermediate vector by inserting the *Eimeria* antigen gene and the dendritic cell-targeting peptide (DCpep) sequence downstream of the AGA2 anchor in the pYD1 plasmid (Fig. 1A). Subsequently, to eliminate the antibiotic-resistance gene, the complete *AmpR* sequence was deleted from the recombinant plasmids via PCR amplification and homologous recombination, generating the final pYD1-*Eimeria* antigen-DCpep ΔAmpR constructs. These constructs rely solely on the *TRP1* auxotrophic marker for selection in the *S. cerevisiae* EBY100 host.

To verify the successful transformation and integrity of the recombinant plasmids, the seven generated yeast strains were lysed, and the resulting lysates were used directly as templates

for PCR amplification. As shown in Fig. 1B, PCR amplification of the insertion regions yielded single, specific bands of the expected sizes for all strains from three independent positive colonies (lanes 1-3). Specifically, the DCpep control strain yielded a 382 bp fragment, while the six antigen-DCpep strains produced fragments (including the DCpep sequence and vector backbone junction) of 1582 bp (*Et*GFAT), 1582 bp (*Et*Sub4), 1282 bp (*Et*AKRO), 880 bp (*Et*GBE), 1357 bp (*Et*α-AMY), and 1648 bp (*Et*4aGT). Furthermore, Sanger sequencing across the deletion site confirmed the complete absence of the *AmpR* gene. These results demonstrate that all target sequences were successfully transformed into the yeast cells and that the *AmpR* gene was completely deleted in all seven recombinant strains.

Expression and surface display of the recombinant fusion proteins

To verify the successful expression and surface localization of the six *E. tenella* sexual-stage candidate antigens, Western blotting and indirect immunofluorescence assays (IFA) were performed on galactose-induced recombinant yeast strains.

As shown in Fig. 2A, distinct immunoreactive bands matching the predicted molecular weights were observed for all six target proteins, as indicated by the red arrows: *Et*GFAT (~68 kDa), *Et*Sub4 (~67 kDa), *Et*AKRO (~56 kDa), *Et*GBE (~40 kDa), *Et*4aGT (~68 kDa), and *Et*α-AMY (~57 kDa). The DCpep control strain exhibited a distinct immunoreactive band, confirming the successful induction of the Aga2p-based display system. Lower-molecular-weight bands detected in the antigen-expressing lanes represent partially degraded or truncated fusion proteins retaining the C-terminal 6×His tag, a common characteristic of the yeast surface-display system.

Next, IFA was performed to confirm cell-surface localization. As shown in Fig. 2B, strong

133 green fluorescence signals were observed on the surface of all six antigen-expressing strains,
134 whereas the DCpep control strain exhibited no detectable fluorescence signal.

135 Finally, to quantify the surface display efficiency, flow cytometric analysis was conducted on
136 the induced strains. As shown in Fig. 3, after gating the intact yeast population (P1) based on
137 FSC-A and SSC-A, the FITC-positive populations (P2 and P3) were analyzed. The DCpep control
138 strain exhibited a very low background fluorescence (0.68%), validating the specificity of the
139 assay. Compared with the control, all six antigen-expressing strains displayed a distinct rightward
140 shift in fluorescence intensity, though with marked antigen-dependent variations in efficiency.
141 Specifically, the surface display efficiencies were 68.04% for *Et*AKRO, 30.90% for *Et*GFAT,
142 23.08% for *Et*α-AMY, 21.76% for *Et*GBE, 18.87% for *Et*4aGT, and 16.73% for *Et*Sub4. These
143 results confirm that while all six fusion proteins were successfully anchored on the yeast surface,
144 their display efficiencies varied significantly, which may be attributed to differences in protein size,
145 spatial conformation, or membrane translocation efficiency.

146 **Antigen-dependent induction of peripheral T-cell and splenic cytokine responses**

147 Prior to the in vivo trial, growth curve analysis revealed that all seven recombinant strains
148 exhibited growth kinetics comparable to the vector control over 72 h of induction, indicating that
149 neither the *AmpR* deletion nor antigen display adversely affected yeast viability (Fig. 4A). The
150 schedule for animal immunization, challenge, and tissue sampling is illustrated in Fig. 4B.

151 To evaluate the cellular immune responses induced by the recombinant yeast vaccines, the
152 proportions of $CD3^+CD4^+$ and $CD3^+CD8^+$ T lymphocyte subsets in the peripheral blood were
153 analyzed by flow cytometry on day 22 (pre-challenge). As shown in Fig. 5, for the $CD3^+CD4^+$ T
154 cells, all immunized groups exhibited significantly higher proportions than the PBS control group .

Notably, the GFAT and Sub4 groups induced significantly higher levels of $CD3^+CD4^+$ T cells than the vector group, whereas the other antigen-immunized groups were comparable to the vector group. Furthermore, the proportion of $CD3^+CD4^+$ T cells in the GFAT group was significantly higher than that in the Sub4 group. For the $CD3^+CD8^+$ T cell subset, a similar trend was observed. Both the GFAT and Sub4 groups exhibited significantly higher proportions compared to the PBS control and the vector control groups, while the remaining antigen groups were comparable to the PBS and vector controls. The GFAT group induced a significantly higher proportion of $CD3^+CD8^+$ T cells than the Sub4 group.

To further evaluate the systemic cytokine milieu, splenic mRNA expression of T-cell-associated cytokines was measured (Fig. 6). Although the vector control significantly upregulated IL-10 compared to the PBS group, the other four cytokines remained at baseline levels. Compared to the vector control, distinct antigen-specific signatures emerged: most antigens (except *Et*AKRO) significantly upregulated IL-2, with *Et*GFAT and *Et*Sub4 showing the highest levels. IL-15 was specifically enhanced by *Et*Sub4 and *Et*4aGT, while IFN-γ was significantly elevated by *Et*Sub4 and *Et*α-AMY. For Th2/regulatory cytokines, IL-4 levels across all antigen groups were comparable to the vector, though *Et*4*aGT* and *Et*α-AMY induced higher IL-4 than *Et*GFAT. Notably, *Et*AKRO uniquely induced the highest IL-10 expression, significantly exceeding the vector control.

Collectively, these results indicate that *Et*GFAT and *Et*Sub4 robustly activated T-cell-mediated immunity, with *Et*GFAT inducing the strongest peripheral response. Additionally, these antigens induced distinct systemic cytokine profiles, with *Et*Sub4 driving a Th1 bias and *Et*GFAT modulating the Th2/regulatory balance.

Histopathological lesions and parasite burden in cecal tissues at day 5 post-challenge

To evaluate the protective effect of the recombinant yeast vaccines, cecal tissues were collected on day 5 post-challenge (day 27 overall) for histopathological examination (H&E staining) and quantification of parasite burden via qPCR.

As shown in Fig. 7A, the PBS control group exhibited normal cecal architecture without visible parasites. In contrast, both the *E. tenella* and vector control groups showed severe mucosal damage, characterized by disrupted villi, epithelial loss, and inflammatory infiltration, with numerous schizonts widely distributed in the mucosa. Notably, all six antigen-vaccinated groups exhibited varying degrees of attenuated lesions and reduced schizont burdens compared to the challenge controls.

To further quantify the parasite burden, qPCR analysis was performed (Fig. 7B). All immunized groups exhibited significantly lower *E. tenella* genomic DNA copy numbers compared to the *E. tenella* Control and Vector groups. Among the vaccine candidates, the GBE group exhibited the most pronounced reduction in parasite burden, followed by the GFAT and Sub4 groups, the AKRO group, and finally the 4aGT and α-AMY groups.

Overall, these results demonstrate that the recombinant yeast vaccines effectively mitigated cecal tissue damage and inhibited parasite replication in vivo.

Recombinant yeast vaccines attenuate cecal inflammatory responses induced by *E. tenella* infection

To investigate the effect of vaccination on local intestinal inflammation, the mRNA expression levels of five pro-inflammatory cytokines (IL-1β, IL-6, IL-8, IL-17, and TNF-α) in the cecal tissues were measured by RT-qPCR on day 8 post-challenge (Fig. 8). Compared with the

199 healthy PBS Control group, the *E. tenella* Control group exhibited significantly upregulated
200 transcription of all five cytokines ($P < 0.05$), confirming that *E. tenella* infection induces a robust
201 local inflammatory response.

202 Notably, compared with the *E. tenella* Control group, the Vector group showed a significantly
203 lower IL-17 level, while no significant differences were observed for the other four cytokines.
204 Compared with the Vector group, the antigen-vaccinated groups revealed varying degrees of
205 inflammatory suppression: IL-1β was significantly reduced in the GFAT, Sub4, 4aGT, and α-AMY
206 groups; IL-6 was significantly reduced in the GFAT group; for IL-8, the GFAT, Sub4, AKRO, and
207 α-AMY groups exhibited significantly lower expression levels; and strikingly, IL-17 expression
208 was significantly reduced in all six antigen-vaccinated groups, reaching levels comparable to the
209 healthy PBS control. The other cytokines in the remaining antigen groups showed no statistically
210 significant differences compared with the Vector group.

211 Overall, these results demonstrate that the recombinant yeast vaccines, particularly GFAT and
212 Sub4, effectively mitigated the local inflammatory immunopathology induced by *E. tenella*
213 infection by suppressing key cytokines such as IL-6, IL-8, and IL-17.

214 **Protective efficacy of the recombinant yeast vaccines against *E. tenella* challenge**

215 To comprehensively evaluate the in vivo protective efficacy of the recombinant yeast
216 vaccines, body weight gain, oocyst output, cecal lesion scores, and the anticoccidial index (ACI)
217 were assessed following *E. tenella* challenge.

218 **Body weight gain:** During the immunization period (Fig. 9A), the GFAT group exhibited a
219 notable increase in body weight gain compared to the healthy PBS control, while the other
220 immunized groups showed body weight gains comparable to the healthy control, indicating no

adverse effects on normal growth. After *E. tenella* challenge (Fig. 9B), the body weight gain in the *E. tenella* control group was significantly lower than that in the healthy PBS control group ($P < 0.05$). Among the immunized groups, the GFAT, GBE, 4aGT, and Sub4 groups exhibited body weight gains comparable to the healthy PBS control, which were slightly higher than the Vector group but without statistical significance. The other antigen groups (AKRO and α-AMY) showed body weight gains comparable to the Vector group and were markedly lower than the healthy control.

Cecal lesions: As shown in Fig. 9C, the GFAT group exhibited significantly lower lesion scores compared with the *E. tenella* control group ($P < 0.05$), but the difference between the GFAT and Vector groups was not statistically significant. The other antigen-immunized groups and the Vector group all had lower lesion scores than the *E. tenella* control group, but these reductions did not reach statistical significance.

Oocyst shedding: Compared with the *E. tenella* control group, all antigen-vaccinated groups exhibited significantly reduced oocyst output ($P < 0.05$). Among them, the GFAT, Sub4, and GBE groups showed significantly lower oocyst output than the vector group (Fig. 9D). Notably, the GFAT and GBE groups achieved oocyst decrease ratios of approximately 50% relative to the *E. tenella* control (Fig. 8E).

Comprehensive anticoccidial index (ACI): As shown in Table 2, four vaccine groups (GFAT, GBE, Sub4, and 4aGT) achieved partial protection (ACI 120–160), whereas AKRO and α-AMY showed no protection, similar to the challenge controls. Notably, GFAT achieved the highest ACI (143), followed by GBE (138), demonstrating that the GFAT vaccine conferred the most favorable comprehensive protection against *E. tenella* infection.

Discussion

The life cycle of *E. tenella* involves a complex interplay between asexual replication and sexual reproduction within the host intestinal epithelium [23]. Traditional vaccines targeting sporozoites or merozoites aim to interrupt the asexual invasion phase; however, their efficacy is often limited because a small number of surviving parasites can still complete the life cycle [3,24]. The sexual phase, encompassing gametocyte development, fertilization, and oocyst wall biogenesis, represents a critical "bottleneck" for parasite transmission [25,26]. Consequently, targeting genes that regulate sexual development and oocyst formation is a highly attractive strategy for transmission-blocking vaccination [7,27].

Building on this rationale, the present study selected six candidate antigens based on their transcriptional upregulation during the sexual stages, although their biological functions vary significantly [28,29]. These antigens are associated with distinct predicted biological processes, including amino sugar biosynthesis, proteolysis, oxidoreductase activity, and carbohydrate metabolism[30]. Among them, *Et*GFAT was prioritized as a core target because it is a well-characterized macrogamete-specific rate-limiting enzyme that catalyzes the formation of glucosamine-6-phosphate, acting as a developmental "switch" for oocyst wall glycosylation [31]. *Et*Sub4, a putative subtilisin-family serine protease, and *Et*AKRO, an aldo-keto reductase, possess partial functional evidence regarding protein processing and immunogenicity [32]. In contrast, *Et*GBE, *Et*4aGT, and *Et*α-AMY represent less-characterized targets; genomic annotations suggest they belong to the amylopectin (starch) metabolic network, which provides energy for sporulation rather than serving as structural components of the oocyst wall [33,34].

Our results demonstrated that the newly constructed *AmpR*-free yeast platform successfully

265 expressed and displayed all six antigens without compromising yeast viability. Interestingly, the
266 flow cytometry data revealed a striking dissociation between surface display efficiency and
267 protective efficacy. The *Et*AKRO strain exhibited the highest proportion of fluorescence-positive
268 yeast cells (68.04%) but conferred limited protection (ACI=118). Conversely, the *Et*Sub4 strain
269 showed the lowest display efficiency (16.73%) yet provided partial protection, while the *Et*GFAT
270 vaccine achieved the highest comprehensive protective efficacy (ACI=143) despite a moderate
271 display efficiency (30.90%). This strongly suggests that the intrinsic immunogenicity and
272 biological function of the antigen, rather than the sheer quantity of protein anchored on the yeast
273 surface, are the decisive factors for inducing protective immunity [14]. Moreover,
274 fluorescence-positive percentages do not directly quantify antigen density, and comparisons across
275 antigens may be affected by differences in antibody recognition.

276 The superior efficacy of the *Et*GFAT vaccine is mechanistically consistent with its essential
277 biological function. As a critical enzyme in the hexosamine pathway, *Et*GFAT orchestrates the
278 synthesis of UDP-GalNAc, a substrate indispensable for oocyst wall glycosylation [10]. A recent
279 study further confirmed that *Et*GFAT is a key regulatory node targeted by the gut microbiota
280 (Intestinimonas) to inhibit parasite gametogenesis [35]. By vaccinating with *Et*GFAT, we may
281 have disrupted this critical structural assembly, leading to defective oocyst formation.

282 In terms of transmission-blocking efficacy, the *Et*GFAT vaccine significantly reduced the
283 total oocyst output by approximately 50% compared with the unimmunized challenged control.
284 Given that oocyst shedding is the primary driver of environmental contamination, this reduction
285 represents a substantial decrease in infection pressure. This immunopathological protection was
286 corroborated by the systemic cellular immune responses: *Et*GFAT vaccination induced the

strongest peripheral $CD3^+CD4^+$ and $CD3^+CD8^+$ T-cell responses, while EtSub4 induced the second highest responses. Furthermore, the splenic cytokine profiles revealed distinct systemic signatures: *Et*Sub4 preferentially drove a Th1-biased response (upregulating IL-2, IL-15, and IFN-γ), whereas *Et*GFAT significantly suppressed the Th2-associated cytokine IL-4 while maintaining IL-10 levels. This robust systemic immunity was accompanied by a significant downregulation of local pro-inflammatory cytokines in the cecum (e.g., IL-1β, IL-6, and IL-8) at day 8 post-challenge, as well as a universal suppression of IL-17 across all antigen-vaccinated groups. By controlling parasite replication early (as evidenced by the reduced parasite DNA load at day 5 post-challenge), the *Et*GFAT vaccine may have prevented the excessive inflammatory cascade that characterizes severe *E. tenella* infection[36].

In contrast to *Et*GFAT and *Et*Sub4, the amylopectin metabolism-related antigens (*Et*GBE, *Et*4aGT, and *Et*α-AMY) exhibited variable protective efficacy. *Et*GBE provided partial protection (ACI=138), whereas *Et*4aGT and *Et*α-AMY showed limited efficacy. Amylopectin metabolism is important for energy storage and parasite development in apicomplexans [37], and alterations in carbohydrate metabolism have been associated with salinomycin resistance in *E. tenella* [38]. This contrast highlights a crucial principle in vaccine design: high sexual-stage transcription alone is insufficient; the target is more likely to be effective if it plays a structural or regulatory role in the transmission bottleneck. Metabolic enzymes, while highly expressed, may not present critical structural vulnerabilities that lead to parasite death when blocked. Furthermore, the reduced oocyst output cannot yet be attributed specifically to direct inhibition of gametogenesis, because suppression of earlier parasite replication could also decrease the number of parasites entering sexual development. Direct assessment of gametocyte abundance, oocyst wall integrity, and the

infectivity of shed oocysts will be required to establish a specific transmission-blocking mechanism [7,17].

Beyond antigen selection, the biosafety of the delivery vector is an important consideration. Although antibiotic resistance markers such as *AmpR* are commonly used during bacterial plasmid propagation, their presence in recombinant microbial vaccines may raise biosafety concerns [39,40]. In this study, we established a safer yeast delivery platform suitable for food-producing animals. While the absence of antibiotic selection pressure raises questions regarding long-term plasmid stability during large-scale fermentation, the robust expression and normal growth observed in our study suggests that the TRP1 auxotrophy provides sufficient selection pressure during the induction phase. It should also be noted that the yeast carrier itself may contribute to immune stimulation through cell-wall components such as β-glucans and mannans [15,41,42]. However, the significant differences observed in immune parameters and protection between the antigen-vaccinated groups and the vector control support an additional, antigen-specific contribution from the displayed parasite antigens [21]. Coupling this *AmpR*-free platform with the DCpep targeting strategy holds great promise for developing environmentally and biologically safe anti-coccidiosis oral vaccines.

However, this study has a few limitations that warrant discussion. First, the overall protection level was partial (maximum ACI of 143), and sterile immunity was not obtained, indicating that targeting a single structural enzyme is insufficient to completely abolish parasite transmission. Future formulations should consider multi-antigen cocktails—such as combining *Et*GFAT with *Et*Sub4 or invasion-blocking antigens-to achieve synergistic, near-complete transmission blockade. Second, although we observed a significant reduction in oocyst output, direct bird-to-bird

transmission experiments were not performed; thus, the exact impact on flock-level transmission requires further verification [43]. Third, the specific contribution of DCpep to dendritic cell targeting requires direct experimental validation, and the precise structural epitopes of *Et*GFAT that trigger the T-cell response remain to be mapped [44].

Conclusions

The study constructed a safe, *AmpR*-free yeast surface-display vaccine platform and identified *Et*GFAT as a highly promising candidate for transmission-blocking vaccines. *Et*GFAT induced enhanced T-cell responses, significantly reduced oocyst shedding, and alleviated cecal immunopathology against *E. tenella*. This study provides a solid experimental foundation for the rational design of recombinant oral vaccines against poultry coccidiosis.

Materials and Methods

Animals, parasite, yeast, and plasmids

One-day-old Sanhuang chickens were obtained from Shanghai Minyou Poultry Breeding Specialized Cooperative (Shanghai, China) and reared under coccidia-free conditions with free access to feed and water. All animal experiments were approved by the Animal Ethics and Welfare Committee of the Shanghai Veterinary Research Institute (approval No. SV-20250916-01) and conducted in accordance with the guidelines for the care and use of laboratory animals.

The *Eimeria tenella* Shanghai strain (resource No. CAAS21111611) was maintained in our laboratory and propagated in coccidia-free chickens as previously described [45,46]. Sporulated oocysts were purified by sucrose density gradient centrifugation and stored in 2.5% potassium dichromate at 4℃ until use. For the preparation of sexual-stage parasites, chickens were infected

with sporulated oocysts, and gamont-enriched fractions were isolated from the cecal mucosa at 132 h post-infection as previously described [47].

Saccharomyces cerevisiae EBY100 (Weidi Biotechnology, Shanghai, China) was used as the host for yeast surface display. The pYD1 vector (Coolaber, Beijing, China), containing the AGA2 anchor, a C-terminal 6×His tag, the TRP1 auxotrophic marker, and the ampicillin-resistance gene (*AmpR*), was used as the backbone.

Construction of pYD1-antigen-DCpep plasmids

Total RNA was extracted from sexual-stage parasites enriched for gamonts using the TRIzol Reagent (Invitrogen, Carlsbad, CA, USA) according to the manufacturer's instructions. RNA concentration and purity were assessed using a NanoDrop 2000 spectrophotometer (Thermo Fisher Scientific, Waltham, MA, USA), and the qualified RNA was reverse-transcribed into cDNA using the HiScript III RT SuperMix for qPCR (Vazyme, Nanjing, China).

Based on the sequences retrieved from the ToxoDB database, DNA fragments encoding the partial coding sequences of the six target antigens were amplified by PCR using the synthesized cDNAs as templates and using specific primers listed in Table 1 and 2×Phabta UniFi Master Mix (Vazyme). Each primer incorporated a 20 bp homology arm complementary to the ends of the linearized vector. Meanwhile, the previously constructed pYD1-DCpep recombinant plasmid was used as the template for PCR amplification to generate a linearized vector backbone. After purification by gel extraction, each *E. tenella* antigen amplicon was assembled with the linearized pYD1-DCpep backbone using the ClonExpress Ultra One Step Cloning Kit V3 (Vazyme) according to the manufacturer’s instructions. A control plasmid, pYD1-DCpep (containing only the DCpep sequence without any antigen fragment), was constructed in parallel. The assembled

products were transformed into *E. coli* DH5α competent cells and screened on LB plates containing 100 μg/mL ampicillin. Individual colonies were cultured, and plasmids were extracted using a plasmid purification kit. The recombinant plasmids were then verified by Sanger sequencing (Sangon Biotech, Shanghai, China).

Deletion of *AmpR* and construction of recombinant *S. cerevisiae* strains

To eliminate the ampicillin resistance gene, two pairs of primers (pYD1-KO-Amp-F1/R1 and pYD1-KO-Amp-F2/R2, Table 1) were designed to amplify the two fragments flanking the *AmpR* region with overlapping sequences at their junctions, using the pYD1-antigen-DCpep plasmids generated in Section 2.2 as templates. The two resulting DNA fragments were purified by gel extraction and reassembled using the ClonExpress Ultra One Step Cloning Kit V3 (Vazyme) to generate the *AmpR*-free circular plasmids.

The assembled products were transformed into competent *S. cerevisiae* EBY100 cells. Following transformation, the cells were recovered in YPD medium at 30℃ with shaking for 2 h. Because the EBY100 host carries a *trp1* mutation and the pYD1 vector contains a functional *TRP1* selection marker, the recovered cells were plated onto synthetic defined medium lacking tryptophan (SD/-Trp) and incubated at 30℃ for 2~3 days to select positive transformants. An vector control strain (EBY100/pYD1-DCpep ΔAmpR) was constructed in parallel using the same strategy.

To verify the successful deletion of *AmpR* and the integrity of the antigen cassettes, single colonies were picked and lysed using the Quick Yeast Positive Clone Assay Kit (Coolaber). The lysates were used as templates for PCR with the pYD1-seq-F/R primers (Table 1). The PCR products were analyzed by agarose gel electrophoresis, and the positive amplicons were further

confirmed by Sanger sequencing (Sangon Biotech). Seven sequence-verified recombinant yeast strains were obtained and designated as EBY100/pYD1-DCpep ΔAmpR, EBY100/pYD1-*Et*GFAT-DCpep ΔAmpR, EBY100/pYD1-*Et*Sub4-DCpep ΔAmpR, EBY100/pYD1-*Et*AKRO-DCpep ΔAmpR, EBY100/pYD1-*Et*GBE-DCpep ΔAmpR, EBY100/pYD1-*Et*4aGT-DCpep ΔAmpR, and EBY100/pYD1-*Et*α-AMY-DCpep ΔAmpR.

Induction and characterization of antigen-displaying yeast strains

The seven recombinant yeast strains were initially cultured in YNB-CAA medium supplemented with 2% glucose at 30℃ with shaking at 200 rpm until the OD_{600} reached 2.0-5.0. To induce target protein expression, the cells were transferred to YNB-CAA medium containing 2% galactose, with the initial OD_{600} adjusted to approximately 1.0. The cultures were then incubated at 30℃ with shaking at 250 rpm for 72 h.

Following induction, 1 mL samples were collected and pelleted by centrifugation. Yeast cells were disrupted and lysed using an ultrasonic cell disruptor, and the protein concentration was determined using a BCA protein assay kit (Beyotime, Shanghai, China). Equal amounts of total protein (10 μg per lane) were separated by 12% SDS-PAGE and transferred onto PVDF membranes (Millipore, Billerica, MA, USA). The membranes were blocked with 5% skim milk in TBST for 1 h at room temperature and incubated overnight at 4 °C with a mouse anti-His-tag monoclonal antibody (1:8000; Proteintech, Wuhan, China). After three washes with TBST, the membranes were incubated with HRP-conjugated goat anti-mouse IgG (1:8000; Proteintech, Wuhan, China) for 1 h at room temperature. Immunoreactive bands were visualized using a chemiluminescent substrate.

For the surface display analysis, induced yeast cells were harvested and washed three times with PBS by centrifugation at 4,000 rpm for 5 min. To ensure the detection of surface-localized antigens, no permeabilization treatment was performed. Cells were fixed with 4% paraformaldehyde for 30 min at room temperature, blocked in PBS containing 3% bovine serum albumin (BSA) for 1 h, and incubated overnight at 4 °C with in-house generated mouse antibodies against the respective antigens (*Et*GFAT, *Et*Sub4, *Et*AKRO, *Et*GBE, *Et*4aGT, or *Et*α-AMY) (1:200 in PBS). After three washes, cells were incubated with FITC-conjugated goat anti-mouse IgG (1:300; Sigma, St. Louis, MO, USA) for 1 h at room temperature in the dark. After three washes, the stained cells were resuspended in a total volume of 200 μL PBS. An aliquot of 4 μL was placed on glass slides and examined under a fluorescence microscope (Nikon, Tokyo, Japan), with bright-field and FITC images captured for each strain. The DCpep control strain was processed identically and used as a negative control. The remaining 196 μL of the cell suspension was analyzed on a Beckman Coulter flow cytometer (Beckman Coulter, Brea, CA, USA). The main yeast population (P1) was gated based on forward scatter (FSC) and side scatter (SSC), excluding debris and cell aggregates, and FITC-positive cells (P2) were gated within P1. The DCpep control strain was used to define background fluorescence, and surface display efficiency was calculated as the percentage of FITC-positive cells within the P1 gate. Three independent induction experiments were performed for each strain.

Growth kinetics of the recombinant yeast strains

To compare the growth characteristics of the recombinant strains with those of the vector control, the seven recombinant strains and the control strain EBY100/pYD1-DCpep ΔAmpR were inoculated separately into YNB-CAA induction medium supplemented with 2% galactose (initial

OD_{600}≈1.0). Cultures were incubated at 30 °C with shaking at 200 rpm. Samples were collected at 12, 24, 36, 48, 60, and 72 h, and the optical density at 600 nm (OD_{600}) was measured using a spectrophotometer. Growth curves were generated by plotting OD_{600} against incubation time. Three independent experiments were performed for each strain.

Preparation of recombinant yeast vaccines

The recombinant yeast strains were induced as previously described, the cells were harvested by centrifugation at 4,000 rpm for 5 min and washed three times with sterile PBS to remove residual medium components. The pelleted yeasts were then resuspended in sterile PBS and quantified using a hemocytometer. The cell suspension was adjusted to a final concentration of 1×10^9 cells/mL and used immediately for oral immunization. Chickens were orally immunized nine times with 1×10^8 cells per dose (in 100 μ L).

Chicken immunization and challenge trial

A total of 108 one-day-old Sanhuang chicks were randomly allocated into nine experimental groups (n=12 per group): six antigen-immunized groups (GFAT, Sub4, AKRO, GBE, 4aGT, and α-AMY), and three control groups: Vector (EBY100/pYD1-DCpep ΔAmpR, challenged), *E. tenella* Control (unimmunized, challenged), and PBS Control (unimmunized, unchallenged). Each chicken in the immunized groups received 100 μL of the yeast suspension (1×10^8 cells) orally on days 1,2,3, 8,9,10, and 15,16,17 after hatching. Chickens in the PBS and *E. tenella* Control groups received an equivalent volume of sterile PBS.

458 At 22 days of age, all chickens except PBS Control group were orally challenged with 20,000
459 freshly sporulated *E. tenella* oocysts. The PBS Control group received an equivalent volume of
460 PBS.

461 **Peripheral blood T-cell subset analysis**

462 Peripheral blood was collected from three randomly selected chickens per group (n=3) on
463 day 22 (immediately before challenge) into EDTA-coated tubes. Single-cell lymphocyte
464 suspensions were isolated using the Chicken Peripheral Blood Lymphocyte Isolation Solution Kit
465 (Solarbio, Beijing, China) according to the manufacturer's instructions. For each sample, cells
466 were divided into two aliquots. One aliquot was incubated with mouse anti-chicken CD3-PE and
467 mouse anti-chicken CD4-FITC antibodies, and the other with mouse anti-chicken CD3-PE and
468 mouse anti-chicken CD8-FITC antibodies (SouthernBiotech, Birmingham, AL, USA) for 30 min
469 at 4℃ in the dark. After washing, samples were analyzed on a Beckman Coulter flow cytometer
470 (Beckman Coulter, Brea, CA, USA). Lymphocytes were gated based on FSC and SSC, and $CD3^+$
471 cells were gated within the lymphocyte population. The proportions of $CD3^+CD4^+$ and $CD3^+CD8^+$
472 T cells were analyzed within the $CD3^+$ population. Data were processed using FlowJo software
473 (Tree Star, Ashland, OR, USA).

474 **Histopathological examination of cecal tissues**

475 On day 27 (5 days post-challenge), three chickens per group (n=3) were randomly selected
476 and humanely euthanized, and cecal tissues were collected. A portion of the tissues was fixed in
477 freshly prepared 10% neutral-buffered formalin and processed using standard histological
478 procedures, including paraffin embedding, sectioning at a thickness of 5 μm, and hematoxylin and
479 eosin (H&E) staining. The stained sections were examined under a light microscope (Olympus,

Tokyo, Japan) to assess the cecal mucosal architecture, tissue damage, inflammatory-cell infiltration, and developmental stages of the parasite. Representative images were captured at 10× and 40× magnification.

Quantification of parasite burden by qPCR

The remaining cecal tissues from day 27 were homogenized with steel beads in lysis buffer using a tissue homogenizer. Genomic DNA was extracted using a Tissue DNA Extraction Kit (Tiangen, Beijing, China) according to the manufacturer's instructions. The *E. tenella* 5S rRNA gene repeat region (*Et*-5S) was selected as the target for quantitative real-time PCR (qPCR) with gene-specific primers (Supplementary Table S1). Real-time PCR was performed on an ABI 7500 system (Applied Biosystems, Foster City, CA, USA). A standard curve was generated using serial 10-fold dilutions of a recombinant plasmid containing the Et-5S fragment. The Et-5S copy number in each sample was calculated from the corresponding cycle threshold (Ct) value using the standard curve. Each sample was analyzed in triplicate, and the results were expressed as Et-5S copies ($\times 10^3$) per reaction.

Cytokine mRNA profiling in the spleen and cecum

The spleen tissues were collected on day 22 (pre-challenge) from the same three chickens used for peripheral blood analysis to detect the mRNA expression of T-cell-associated cytokines (IL-2, IL-4, IL-10, IL-15, and IFN-γ). Similarly, cecal tissues were collected on day 30 (8 days post-challenge) from another three randomly selected chickens per group (n=3) to detect the mRNA expression of pro-inflammatory cytokines (IL-1β, IL-6, IL-8, IL-17, and TNF-α).

All collected tissues were immediately snap-frozen in liquid nitrogen and stored at −80 °C until further analysis. Total RNA was extracted separately from the spleen and cecal tissues using TRIzol Reagent (Invitrogen) according to the manufacturer's instructions, and cDNA was synthesized using HiScript III RT SuperMix for qPCR (Vazyme). Quantitative real-time PCR (qPCR) was performed using the chicken β-actin gene as the internal reference. Relative gene expression levels were calculated using the $2^{-\Delta\Delta Ct}$ method, with the corresponding uninfected PBS control group as the calibrator. The primer sequences and expected amplicon sizes are provided in Supplementary Table S1.

Evaluation of protective efficacy against *E. tenella* challenge

The protective efficacy of the recombinant yeast vaccines was evaluated based on body-weight gain, survival rate, oocyst shedding, and cecal lesion severity. Body weights of all chickens were individually recorded on days 1 (baseline), 22 (before challenge), and 30 (end of the experiment). Body-weight gain during the immunization period was calculated as the difference between day 22 and day 1, while body-weight gain during the challenge period was calculated as the difference between day 30 and day 22. Fecal samples were collected from the surviving chickens in each group from days 6 to 8 post-challenge. Oocyst output was determined using the McMaster counting technique. Three technical replicate counts were performed for each group, and the number of oocysts per gram of feces (OPG) was determined. The oocyst decrease ratio (%) was calculated as: (mean OPG of the *E. tenella* Control group − mean OPG of the immunized group)/mean OPG of the *E. tenella* Control group × 100%. Cecal lesion severity was scored on day 30 using a 0–4 scoring system as described by Johnson and Reid [48].

The anticoccidial index (ACI) was calculated using the following formula: ACI=survival rate (%)＋relative body weight gain (%)－oocyst value－cecal lesion value, where the oocyst value and cecal lesion value were assigned according to the standard scoring criteria described by De Pablos et al [49]. Relative body-weight gain (%) was calculated as: (mean body-weight gain of the immunized group / mean body-weight gain of the PBS Control group) × 100%. An ACI below 120 indicated no protection, 120–160 indicated partial protection, and above 160 indicated strong protection.

Statistical analysis

All experimental data are presented as mean±standard error of the mean (SEM). Statistical analysis was conducted using GraphPad Prism (version 9.0; GraphPad Software, San Diego, CA, USA). For multiple comparisons, one-way analysis of variance (ANOVA) followed by Tukey's post hoc test was performed. For ordinal cecal lesion scores, the Kruskal–Wallis test followed by Dunn's post hoc test was applied. Differences were considered statistically significant at $P < 0.05$.

Data availability

No datasets were generated or analysed during the current study.

Acknowledgements

Not applicable.

Funding

This work was supported by the Key Research and Development of Science and Technology Plan in Tibet Autonomous Region (XZ202401ZY0052), National Key Research and Development Program of China (Grant No. 2023YFD1802400), National Natural Science Foundation of China (Grant No. 32373038), and the National Parasitic Resources Center (NPRC-2019-194-30).

Author information

Authors and Affiliations

Shanghai Veterinary Research Institute, Chinese Academy of Agricultural Sciences, Minhang, Shanghai, 200241, PR China

Jinwen Wang, Yan Cai, Qiping Zhao, Shunhai Zhu, Yu Yu, Jiayu Bai, Wenqi Han, Shanbo Wu, Fanghe Zhao, Hongyu Han, Hui Dong

College of Animal Husbandry and Veterinary Medicine, Southwest Minzu University, Chengdu, 610041, PR China

Yan Cai

Animal, Plant and Food Inspection Center of Nanjing Customs District, Nanjing 210001, PR China

Zhen Feng

Contributions

Jinwen Wang: Validation, Visualization, Writing-original draft, Writing-review & editing, Conceptualization. Yan Cai: Writing-review & editing, Writing-original draft. Zhen Feng: Resources, Investigation. Qiping Zhao: Investigation, Investigation, Data curation. Shunhai Zhu: Investigation. Yu Yu: Investigation. Jiayu Bai: Resources. Wenqi Han: Data curation. Shanbo Wu: Software. Fanghe Zhao: Formal analysis. Hongyu Han: Supervision, Resources, Investigation. Hui Dong: Supervision, Resources, Investigation.

Corresponding author

Correspondence to Hui Dong or Hongyu Han.

Ethics declarations

Ethics approval and consent to participate

All animal experiments were approved by the Animal Ethics and Welfare Committee of the Shanghai Veterinary Research Institute (approval No. SV-20250916-01).

Consent for publication

Not applicable.

Competing interests

All authors declare that they have no financial or non-financial competing interests.

Supplementary Information

References

1. Blake DP, Knox J, Dehaeck B, Huntington B, Rathinam T, Ravipati V, Ayoade S, Gilbert W, Adebambo AO, Jatau ID, Raman M, Parker D, Rushton J, Tomley FM. Re-calculating the cost of coccidiosis in chickens. Vet Res. 2020;51:115. https://doi.org/10.1186/s13567-020-00837-2

2. Chapman HD, Rathinam T. Focused review: The role of drug combinations for the control of coccidiosis in commercially reared chickens. International Journal for Parasitology: Drugs and Drug Resistance. 2022;18:32–42. https://doi.org/10.1016/j.ijpddr.2022.01.001

3. Shirley MW, Smith AL, Tomley FM. The biology of avian *Eimeria* with an emphasis on their control by vaccination. Adv Parasitol. 2005;60:285–330. https://doi.org/10.1016/S0065-308X(05)60005-X

4. Sharman PA, Smith NC, Wallach MG, Katrib M. Chasing the golden egg: vaccination against poultry coccidiosis. Parasite Immunol. 2010;32(8):590–8. https://doi.org/10.1111/j.1365-3024.2010.01209.x

5. Tomley FM, Soldati DS. Mix and match modules: structure and function of microneme proteins

587 in apicomplexan parasites. Trends in Parasitology. Elsevier; 2001;17:81–8.
588 https://doi.org/10.1016/S1471-4922(00)01761-X
589 6. Cowper B, Matthews S, Tomley F. The molecular basis for the distinct host and tissue tropisms
590 of coccidian parasites. Molecular and Biochemical Parasitology. 2012;186:1–10.
591 https://doi.org/10.1016/j.molbiopara.2012.08.007
592 7. Wallach M. The importance of transmission-blocking immunity in the control of infections by
593 apicomplexan parasites. International Journal for Parasitology. 1997;27:1159–67.
594 https://doi.org/10.1016/S0020-7519(97)00113-6
595 8. Wallach M, Pillemer G, Yarus S, Halabi A, Pugatsch T, Mencher D. Passive immunization of
596 chickens against *Eimeria maxima* infection with a monoclonal antibody developed against a
597 gametocyte antigen. Infect Immun. 1990;58:557–62. https://doi.org/10.1128/iai.58.2.557-562.1990
598 9. Williams RB. Anticoccidial vaccines for broiler chickens: pathways to success. Avian Pathol.
599 2002;31(4):317–53. https://doi.org/10.1080/03079450220148988
600 10. Belli SI, Wallach MG, Smith NC. Cloning and characterization of the 82 kDa tyrosine-rich
601 sexual stage glycoprotein, GAM82, and its role in oocyst wall formation in the apicomplexan
602 parasite, *Eimeria maxima*. Gene. 2003;307:201–12.
603 https://doi.org/10.1016/S0378-1119(03)00451-7
604 11. Walker RA, Sharman PA, Miller CM, Lippuner C, Okoniewski M, Eichenberger RM,
605 Ramakrishnan C, Brossier F, Deplazes P, Hehl AB, Smith NC. RNA Seq analysis of the *Eimeria*
606 *tenella* gametocyte transcriptome reveals clues about the molecular basis for sexual reproduction
607 and oocyst biogenesis. BMC Genomics. 2015;16:94. https://doi.org/10.1186/s12864-015-1298-6
608 12. Rafiqi SI, Garg R, Ram H, Reena KK, Asari M, Kumari P, Kundave VR, Singh M, Banerjee

609 PS. Immunoprophylactic evaluation of recombinant gametocyte 22 antigen of *Eimeria tenella* in
610 broiler chickens. Parasitol Res. 2019;118(3):945–53. https://doi.org/10.1007/s00436-018-06198-2
611 13. Wiedmer S, Alnassan AA, Volke B, Thabet A, Daugschies A, Lendner M, Kurth M. Passive
612 immunization with *Eimeria tenella* gametocyte antigen 56 (*Et*GAM56) specific antibodies and
613 active immunization trial with the epitope containing peptide. Vet Parasitol. 2017;247:100–7.
614 https://doi.org/10.1016/j.vetpar.2017.09.019
615 14. Boder ET, Wittrup KD. Yeast surface display for screening combinatorial polypeptide libraries.
616 Nat Biotechnol. 1997;15:553–7. https://doi.org/10.1038/nbt0697-553
617 15. Brown GD, Gordon S. Immune recognition. A new receptor for beta-glucans. Nature.
618 2001;413:36–7. https://doi.org/10.1038/35092620
619 16. Sun H, Wang L, Wang T, Zhang J, Liu Q, Chen P, et al. Display of *Eimeria tenella Et*Mic2
620 protein on the surface of Saccharomyces cerevisiae as a potential oral vaccine against chicken
621 coccidiosis. Vaccine. 2014;32:1869–76. https://doi.org/10.1016/j.vaccine.2014.01.068
622 17. Soutter F, Werling D, Nolan M, Küster T, Attree E, Marugán-Hernández V, et al. A Novel
623 Whole Yeast-Based Subunit Oral Vaccine Against *Eimeria tenella* in Chickens. Front Immunol.
624 2022;13. https://doi.org/10.3389/fimmu.2022.809711
625 18. Han W, Chen L, Wang L, Zhao Q, Zhu S, Yu Y, et al. A yeast-based oral vaccine platform
626 reveals antigen-dependent protection against *Eimeria tenella*. Poultry Science. 2026;105:107401.
627 https://doi.org/10.1016/j.psj.2026.107401
628 19. Yang G, Yao J, Yang W, Jiang Y, Du J, Huang H, et al. Construction and immunological
629 evaluation of recombinant Lactobacillus plantarum expressing SO7 of *Eimeria tenella* fusion
630 DC-targeting peptide. Veterinary Parasitology. 2017;236:7–13.

631 https://doi.org/10.1016/j.vetpar.2017.01.023

632 20. Chen W, Ma C, Wang D, Li G, Ma D. Immune response and protective efficacy of

633 recombinant Enterococcus faecalis displaying dendritic cell-targeting peptide fused with *Eimeria*

634 *tenella* 3-1E protein. Poult Sci. 2020;99(6):2967–75. https://doi.org/10.1016/j.psj.2020.03.014

635 21. Curiel TJ, Morris C, Brumlik M, Landry SJ, Finstad K, Nelson A, Joshi V, Hawkins C, Alarez

636 X, Lackner A, Mohamadzadeh M. Peptides identified through phage display direct immunogenic

637 antigen to dendritic cells. J Immunol. 2004;172(12):7425–31.

638 https://doi.org/10.4049/jimmunol.172.12.7425

639 22. García-Calvo L, Kummen C, Rustad S, Rønning SB, Fagerlund A. A toolkit for facilitating

640 markerless integration of expression cassettes in Komagataella phaffii via CRISPR/Cas9. Microb

641 Cell Fact. 2025;24:97. https://doi.org/10.1186/s12934-025-02716-x

642 23. Walker RA, Ferguson DJP, Miller CMD, Smith NC. Sex and Eimeria: a molecular perspective.

643 Parasitology. 2013;140(14):1701–17. https://doi.org/10.1017/S0031182013000838

644 24. Blake DP, Knox J, Dehaeck B, Huntington B, Rathinam T, Ravipati V, et al. Re-calculating the

645 cost of coccidiosis in chickens. Vet Res. 2020;51:115. https://doi.org/10.1186/s13567-020-00837-2

646 25. Ramakrishnan C, Smith NC. Recent achievements and doors opened for coccidian parasite

647 research and development through transcriptomics of enteric sexual stages. Molecular and

648 Biochemical Parasitology. 2021;243:111373. https://doi.org/10.1016/j.molbiopara.2021.111373

649 26. Belli SI, Smith NC, Ferguson DJP. The coccidian oocyst: a tough nut to crack! Trends in

650 Parasitology. Elsevier; 2006;22:416–23. https://doi.org/10.1016/j.pt.2006.07.004

651 27. Sharman PA, Smith NC, Wallach MG, Katrib M. Chasing the golden egg: vaccination against

652 poultry coccidiosis. Parasite Immunol. 2010;32(8):590–8.

653 https://doi.org/10.1111/j.1365-3024.2010.01209.x.

654 28. Belli SI, Wallach MG, Luxford C, Davies MJ, Smith NC. Roles of Tyrosine-Rich Precursor
655 Glycoproteins and Dityrosine- and 3,4-Dihydroxyphenylalanine-Mediated Protein Cross-Linking
656 in Development of the Oocyst Wall in the Coccidian Parasite *Eimeria maxima*. Eukaryot Cell.
657 2003;2:456–64. https://doi.org/10.1128/EC.2.3.456-464.2003

658 29. Belli SI, Ferguson DJP, Katrib M, Slapetova I, Mai K, Slapeta J, et al. Conservation of
659 proteins involved in oocyst wall formation in *Eimeria maxima*, *Eimeria tenella* and *Eimeria*
660 *acervulina*. Int J Parasitol. 2009;39:1063–70. https://doi.org/10.1016/j.ijpara.2009.05.004

661 30. Belli SI, Wallach MG, Smith NC. Cloning and characterization of the 82 kDa tyrosine-rich
662 sexual stage glycoprotein, GAM82, and its role in oocyst wall formation in the apicomplexan
663 parasite, *Eimeria maxima*. Gene. 2003;307:201–12.
664 https://doi.org/10.1016/S0378-1119(03)00451-7

665 31. Walker RA, Slapetova I, Slapeta J, Miller CM, Smith NC. The Glycosylation Pathway of
666 *Eimeria tenella* Is Upregulated during Gametocyte Development and May Play a Role in Oocyst
667 Wall Formation. Eukaryot Cell. 2010;9:127–35. https://doi.org/10.1128/EC.00255-09

668 32. Katrib M, Ikin RJ, Brossier F, Robinson M, Slapetova I, Sharman PA, et al. Stage-specific
669 expression of protease genes in the apicomplexan parasite, *Eimeria tenella*. BMC Genomics.
670 2012;13:685. https://doi.org/10.1186/1471-2164-13-685

671 33. Sugi T, Tu V, Ma Y, Tomita T, Weiss LM. *Toxoplasma gondii* Requires Glycogen
672 Phosphorylase for Balancing Amylopectin Storage and for Efficient Production of Brain Cysts.
673 mBio. 2017;8:e01289-17. https://doi.org/10.1128/mBio.01289-17

674 34. Belli SI, Witcombe D, Wallach MG, Smith NC. Functional genomics of gam56:

675 characterisation of the role of a 56 kilodalton sexual stage antigen in oocyst wall formation in
676 *Eimeria maxima*. Int J Parasitol. 2002;32:1727–37.
677 https://doi.org/10.1016/s0020-7519(02)00212-6
678 35. Li J-Y, Huang H-B, Shi C-W, Pan T-X, Li M-H, Wang N, et al. Increased caecal
679 Intestinimonas abundance inhibits E. tenella gametogenesis via EtGFAT regulation and alleviates
680 infection through immunity. Microbiome. 2026;14:62.
681 https://doi.org/10.1186/s40168-025-02302-8
682 36. Wallach M. Role of antibody in immunity and control of chicken coccidiosis. Trends in
683 Parasitology. Elsevier; 2010;26:382–7. https://doi.org/10.1016/j.pt.2010.04.004
684 37. Sugi T, Tu V, Ma Y, Tomita T, Weiss LM. *Toxoplasma gondii* Requires Glycogen
685 Phosphorylase for Balancing Amylopectin Storage and for Efficient Production of Brain Cysts.
686 mBio. 2017;8:e01289-17. https://doi.org/10.1128/mBio.01289-17
687 38. Yu Y, Dong H, Zhao Q, Zhu S, Wang H, Yao Y, et al. Combined transcriptome and whole
688 genome sequencing analyses reveal candidate drug-resistance genes of *Eimeria tenella*. iScience.
689 2024;28:111592. https://doi.org/10.1016/j.isci.2024.111592
690 39. Kumar R, Kumar P. Yeast-based vaccines: New perspective in vaccine development and
691 application. FEMS Yeast Res. 2019;19:foz007. https://doi.org/10.1093/femsyr/foz007
692 40. Han B, Yue F, Zhang X, Xu K, Zhang Z, Sun Z, et al. Genetically engineering of
693 Saccharomyces cerevisiae for enhanced oral delivery vaccine vehicle. Fish & Shellfish
694 Immunology. 2024;146:109425. https://doi.org/10.1016/j.fsi.2024.109425
695 41. Brown GD, Taylor PR, Reid DM, Willment JA, Williams DL, Martinez-Pomares L, et al.
696 Dectin-1 Is A Major β-Glucan Receptor On Macrophages. J Exp Med. 2002;196:407–12.

https://doi.org/10.1084/jem.20020470

42. Brown GD. Dectin-1: a signalling non-TLR pattern-recognition receptor. Nat Rev Immunol. 2006;6(1):33–43. https://doi.org/10.1038/nri1745

43. Wallach MG, Ashash U, Michael A, Smith NC. Field Application of a Subunit Vaccine against an Enteric Protozoan Disease. PLoS One. 2008;3:e3948. https://doi.org/10.1371/journal.pone.0003948

44. Curiel TJ, Morris C, Brumlik M, Landry SJ, Finstad K, Nelson A, Joshi V, Hawkins C, Alarez X, Lackner A, Mohamadzadeh M. Peptides identified through phage display direct immunogenic antigen to dendritic cells. J Immunol. 2004;172(12):7425–31. https://doi.org/10.4049/jimmunol.172.12.7425

45. Ryley JF, Meade R, Hazelhurst J, Robinson TE. Methods in coccidiosis research: separation of oocysts from faeces. Parasitology. 1976;73:311–26. https://doi.org/10.1017/s0031182000046990

46. Jiang L, Zhao Q, Zhu S, Han H, Dong H, Huang B. Establishment of *Eimeria tenella* (local isolate) in chicken embryos. Parasite. 2012;19:285–9. https://doi.org/10.1051/parasite/2012193285

47. Chen L, Tang X, Sun P, Hu D, Zhang Y, Wang C, et al. Comparative transcriptome profiling of *Eimeria tenella* in various developmental stages and functional analysis of an ApiAP2 transcription factor exclusively expressed during sporogony. Parasit Vectors. 2023;16:241. https://doi.org/10.1186/s13071-023-05828-8

48. Johnson J, Reid WM. Anticoccidial drugs: lesion scoring techniques in battery and floor-pen experiments with chickens. Exp Parasitol. 1970;28:30–6. https://doi.org/10.1016/0014-4894(70)90063-9

719 49. De Pablos LM, dos Santos MFB, Montero E, Garcia-Granados A, Parra A, Osuna A.

720 Anticoccidial activity of maslinic acid against infection with *Eimeria tenella* in chickens. Parasitol

721 Res. 2010;107(3):601 – 4. https://doi.org/10.1007/s00436-010-1901-3

722 **Figure legends**

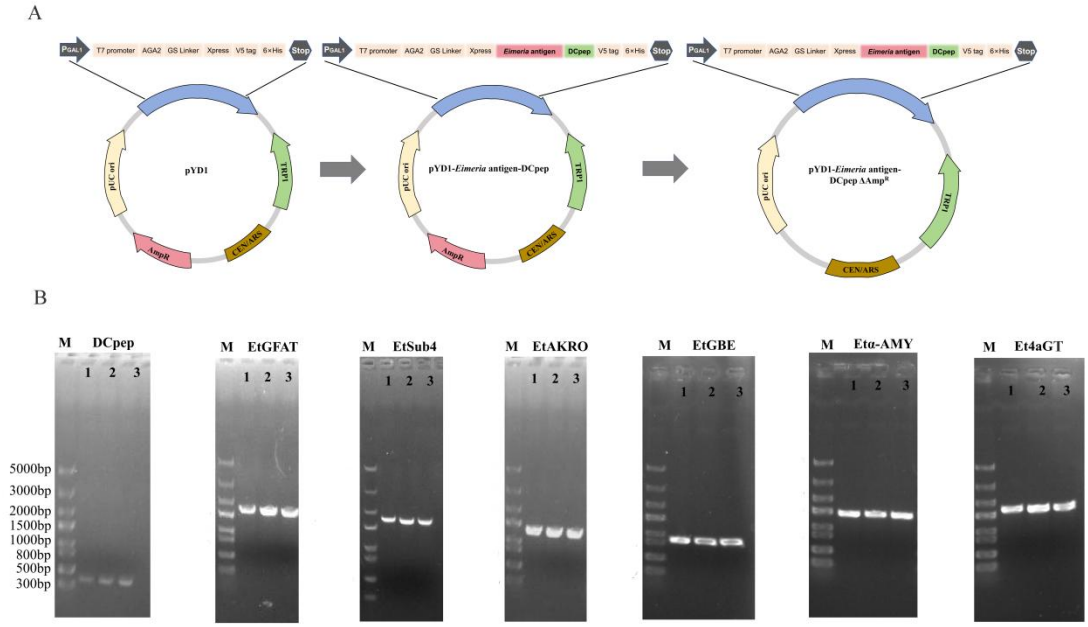

723

724 **Fig. 1. Construction and identification of AmpR-free recombinant *S. cerevisiae* strains.**

725 (A) Schematic representation of the plasmid construction. The *Eimeria* antigen and DCpep

726 sequences were cloned downstream of the AGA2 anchor in the pYD1 vector. The complete

727 AmpR gene was subsequently deleted by PCR to generate the pYD1-*Eimeria* antigen-DCpep

728 ΔAmpR constructs. (B) PCR identification of the seven recombinant strains. M: DNA molecular

729 weight marker (5000, 3000, 2000, 1500, 1000, 800, 500, 300 bp). For each strain, three

730 independent positive colonies (lanes 1–3) were verified. All strains were based on the

731 EBY100/pYD1-antigen-DCpep ΔAmpR backbone. The expected amplicon sizes are 382 bp

732 (DCpep), 1582 bp (*Et*GFAT), 1582 bp (*Et*Sub4), 1282 bp (*Et*AKRO), 880 bp (*Et*GBE), 1357 bp

733 (*Et*α-AMY), and1648 bp (*Et*4aGT).

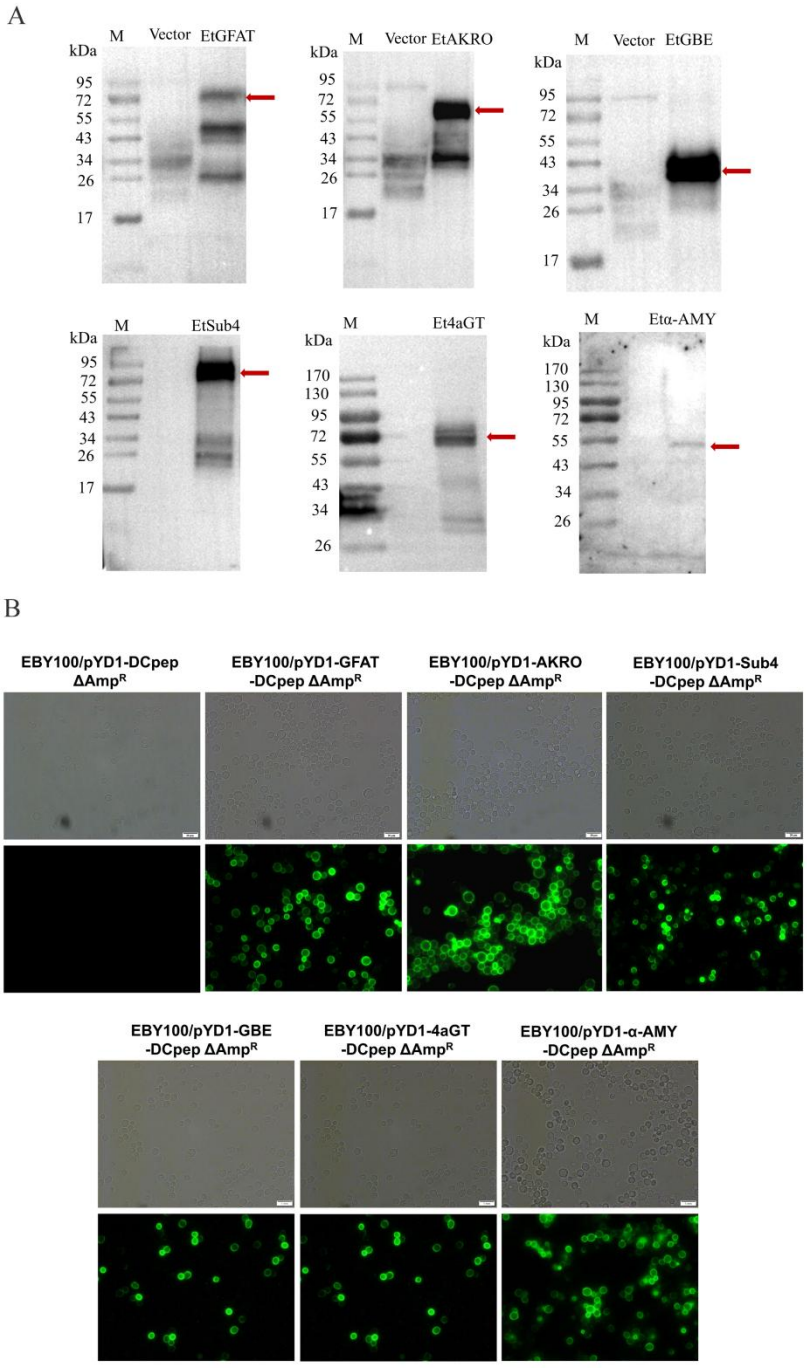

734

735 **Fig. 2. Expression and surface display of the six *E. tenella* antigen–DCpep fusion proteins in**

736 **recombinant *S. cerevisiae* strains.**

737 **(A)** Western blot analysis of total protein extracts from galactose-induced yeast cells using a

738 mouse anti-His monoclonal antibody. The specific full-length target proteins are indicated by red

739 arrows. Because the identical vector strain (EBY100/pYD1-DCpep ΔAmpR) was used across all

740 experiments, three representative control blots are displayed alongside the top row; these controls
741 apply equally to the bottom row. **(B)** Indirect immunofluorescence assay (IFA) of the recombinant
742 yeast strains. The top panels show bright-field images, and the bottom panels show FITC
743 fluorescence (green), indicating the surface display of the target antigens. The vector control strain
744 (EBY100/pYD1-DCpep Δ*AmpR*) shows no specific fluorescence. Scale bars, 20 μm.

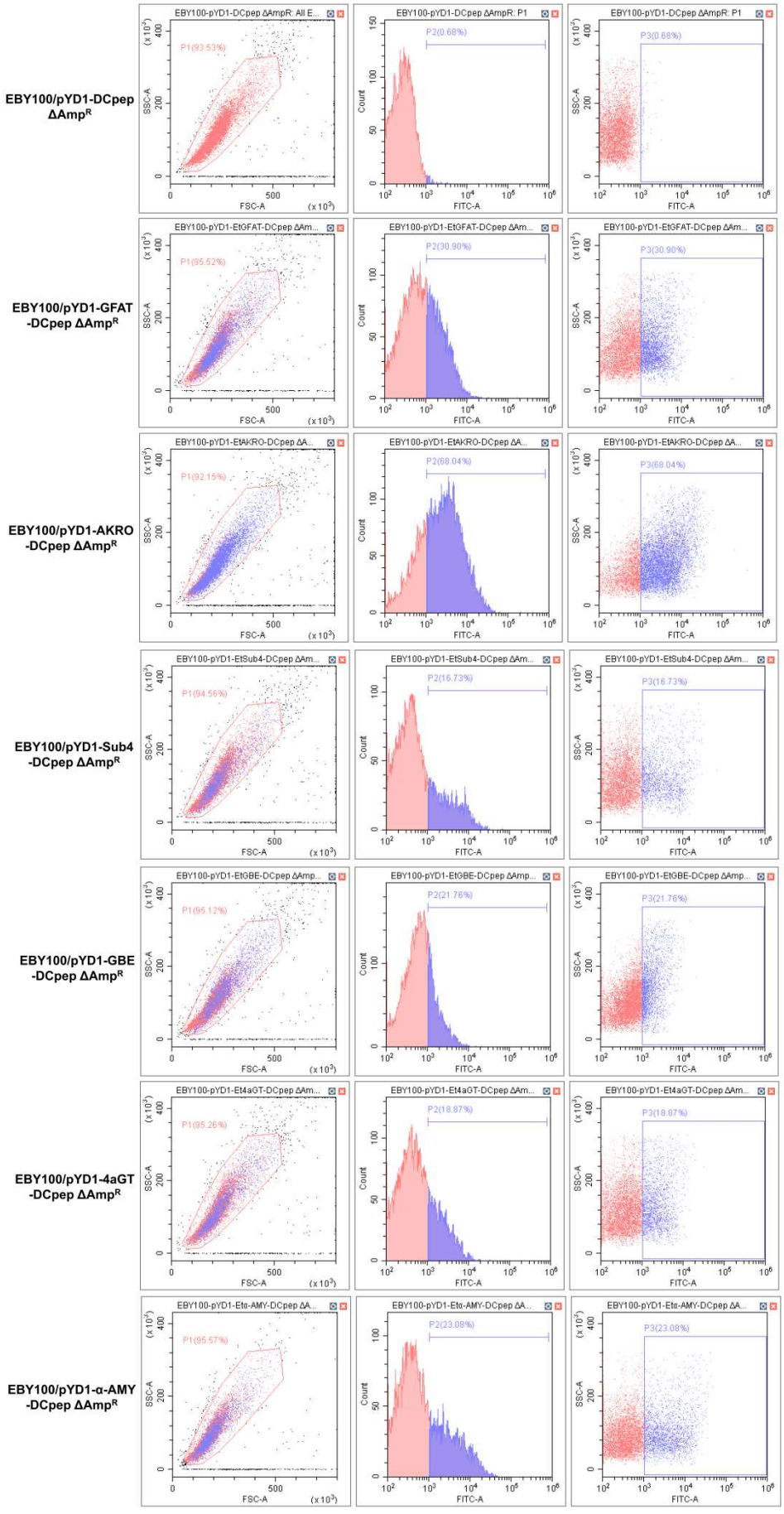
EBY100/pYD1-DCpep ΔAmpR
EBY100/pYD1-GFAT -DCpep ΔAmpR
EBY100/pYD1-AKRO -DCpep ΔAmpR
EBY100/pYD1-Sub4 -DCpep ΔAmpR
EBY100/pYD1-GBE -DCpep ΔAmpR
EBY100/pYD1-4aGT -DCpep ΔAmpR
EBY100/pYD1-α-AMY -DCpep ΔAmpR
SSC-A
FSC-A
Count
FITC-A

745

Fig. 3. Flow cytometric analysis of the surface display efficiency of the six *E. tenella* antigens on recombinant *S. cerevisiae*.

The induced yeast cells were stained with six in-house generated mouse antibodies specific to the respective *Eimeria* antigens, followed by FITC-conjugated secondary antibodies. For each strain, the left panel shows the gating strategy (P1) to select intact yeast cells based on FSC-A vs. SSC-A; the middle panel shows the fluorescence intensity histogram, and the right panel shows the SSC-A vs. FITC-A scatter plot. The percentages of FITC-positive cells (P2 and P3 gates) represent the surface display efficiency of the respective antigens.

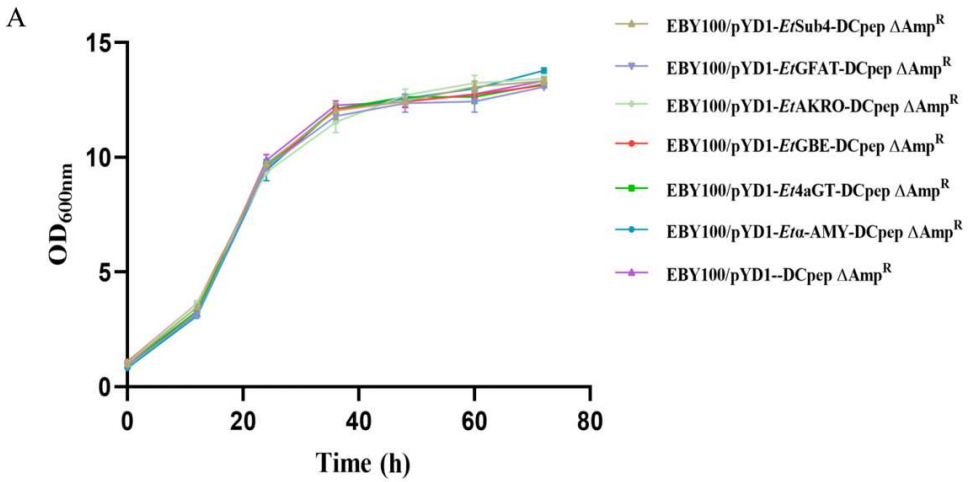

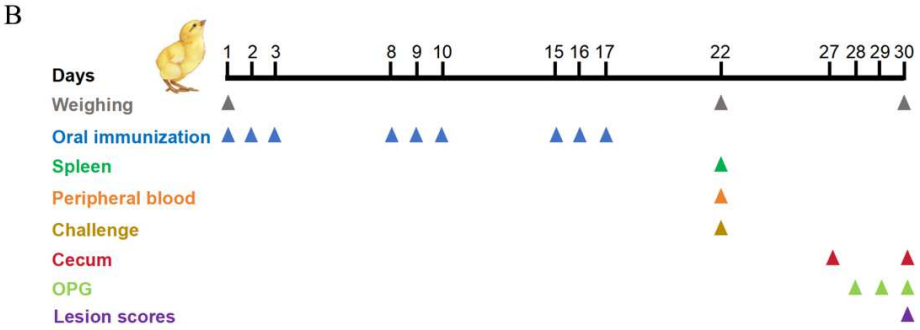

Fig. 4. Growth kinetics of recombinant yeast strains and the schedule of the animal trial.

(A) Growth curves of the seven recombinant *S. cerevisiae* strains in YNB-CAA induction medium

containing 2% galactose over 72 h. The optical density at 600 nm (OD_{600}) was measured every 12 h. Data are presented as mean ± SEM of three independent experiments. (B) Schematic timeline of the chicken immunization and challenge trial. Colored markers indicate the specific time points for weighing (grey), oral immunization (blue), sample collections [peripheral blood (orange), spleen (green), and cecum (red), *E. tenella* challenge (yellow), oocyst output (OPG, light green), and lesion scoring (purple).

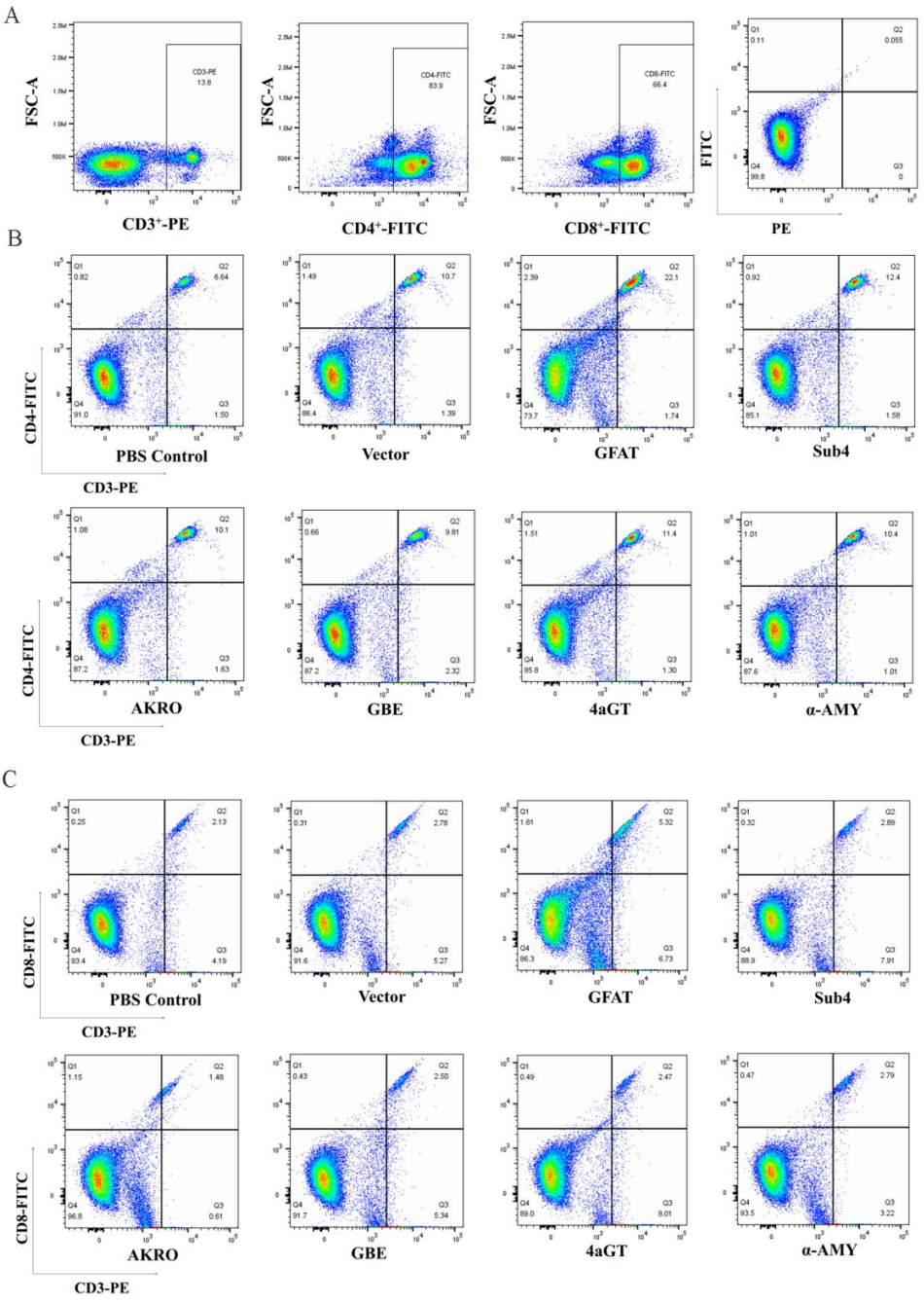
A
FSC-A
CD3⁺-PE
CD4⁺-FITC
CD8⁺-FITC
FITC
PE
B
CD4-FITC
CD3-PE
PBS Control
Vector
GFAT
Sub4
AKRO
GBE
4aGT
α-AMY
C
CD8-FITC
CD3-PE
PBS Control
Vector
GFAT
Sub4
AKRO
GBE
4aGT
α-AMY
D
% of CD3⁺CD4⁺ and CD3⁺CD8⁺ T cells
PBS Control
Vector
GFAT
Sub4
AKRO
GBE
4aGT
α-AMY
CD3⁺CD4⁺ T cell
CD3⁺CD8⁺ T cell

763

Fig. 5. Flow cytometric analysis of peripheral blood T lymphocyte subsets after immunization.

Peripheral blood was collected on day 22 (pre-challenge; 5 days after the third immunization). **(A)** Gating strategy for the identification of $CD3^+$, $CD3^+CD4^+$, and $CD3^+CD8^+$ T cells. **(B, C)** Representative flow cytometry scatter plots showing the percentages of $CD3^+CD4^+$ T cells (Q2 quadrant) and $CD3^+CD8^+$ T cells (Q2 quadrant) across different groups. **(D)** Statistical analysis of the percentages of $CD3^+CD4^+$ and $CD3^+CD8^+$ T cells in peripheral blood. Data are presented as mean ± SEM. Different lowercase letters (a, b, c,) above the bars indicate significant differences between groups ($P < 0.05$).

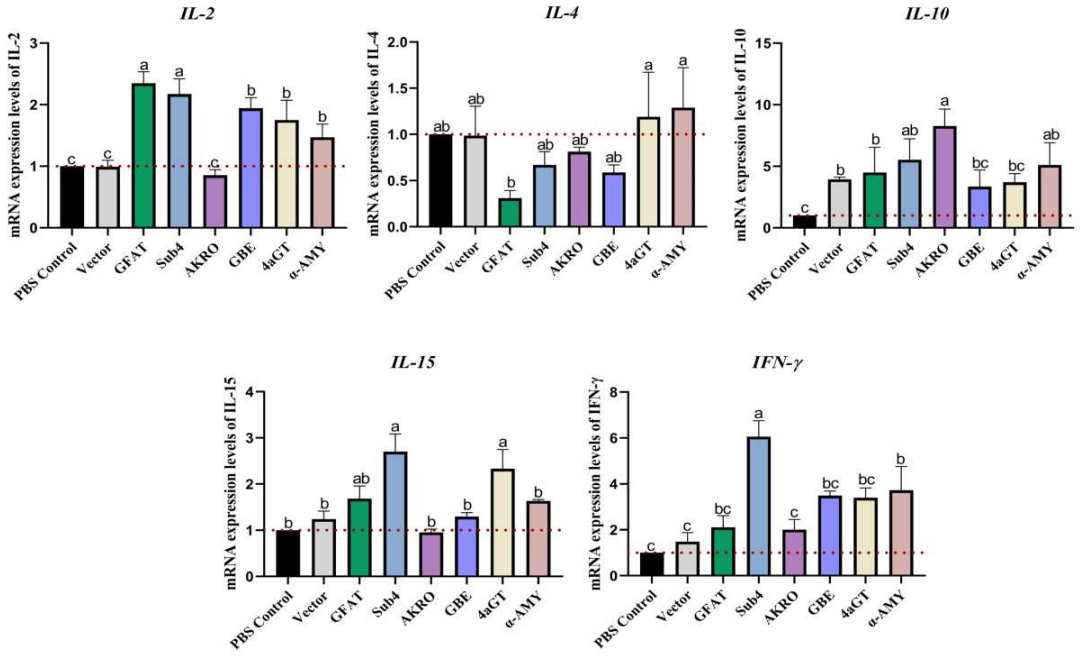

Fig. 6. Effects of recombinant yeast vaccines on splenic T-cell-associated cytokine mRNA expression.

The relative mRNA expression levels of IL-2, IL-4, IL-10, IL-15, and *IFN-γ* in the spleen were measured by RT-qPCR on day 22 (pre-challenge). The PBS control group served as the calibrator (indicated by the red dashed line). Data are presented as the mean ± SEM (n = 3). Different

779 lowercase letters (a, b, c) above the bars indicate statistically significant differences among groups

780 ($P < 0.05$).

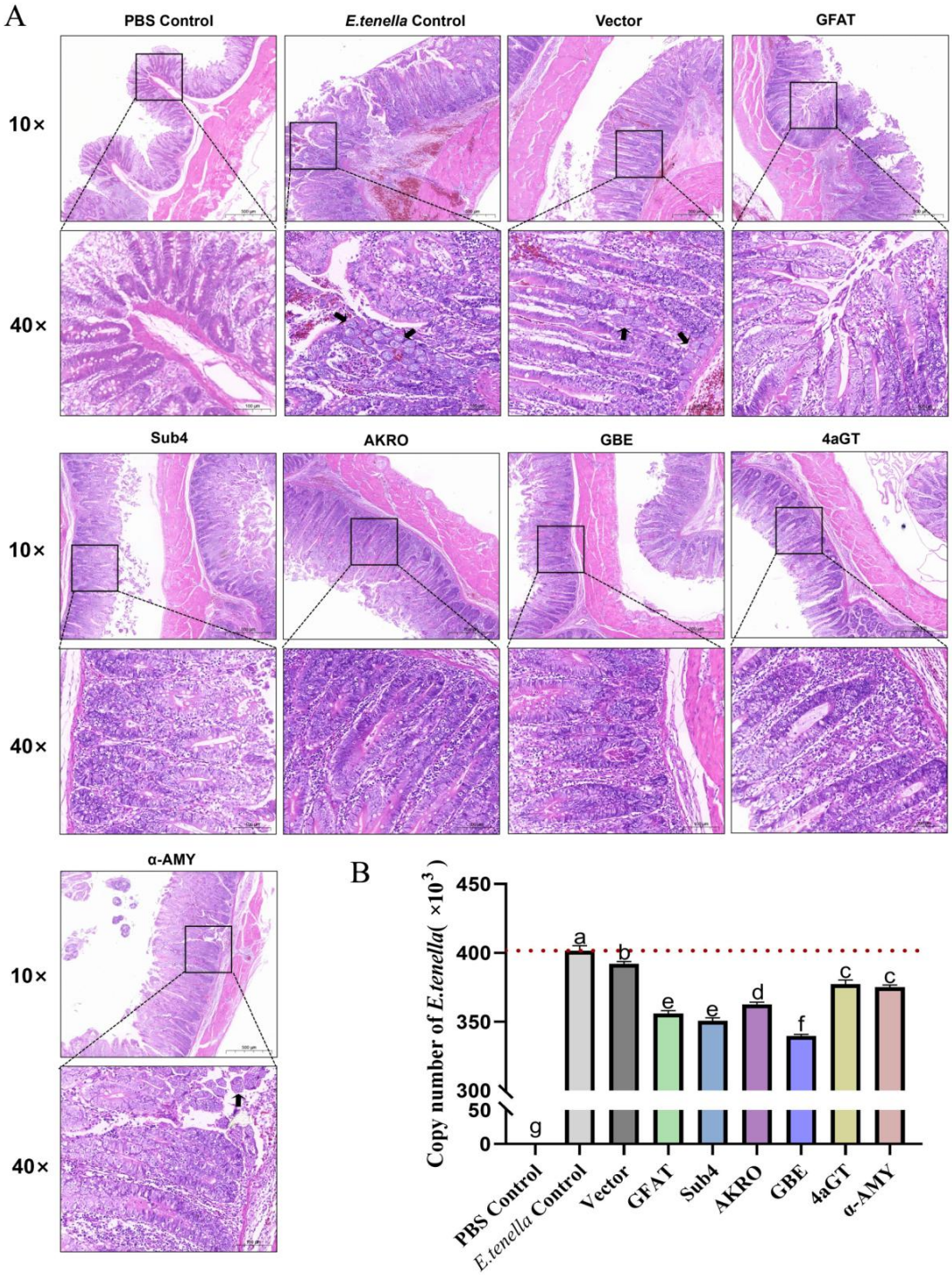

781

782 **Fig. 7. Histopathological changes and parasite burden in cecal tissues after *E. tenella***

783 **challenge.**

(A) Representative H&E-stained cecal tissue sections from different groups at 10× (top panels) and 40× (bottom panels, magnified from the black boxes) magnification. Black arrows indicate *E. tenella* schizonts. Scale bars: 500 μm (10×) and 100 μm (40×).

(B) Quantification of *E. tenella* genomic DNA copies in cecal tissues by qPCR. Data are presented as mean ± SEM. Different lowercase letters (a–g) indicate significant differences between groups ($P < 0.05$).

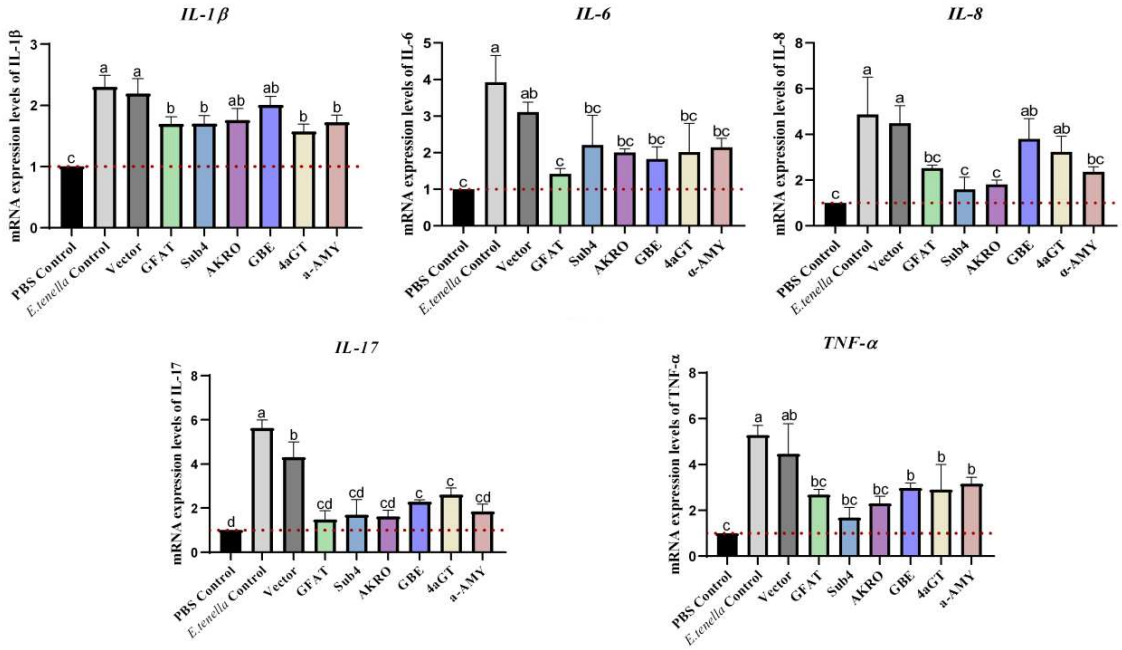

Fig. 8. Effect of recombinant yeast vaccines on the mRNA expression of pro-inflammatory cytokines in cecal tissues after *E. tenella* challenge.

The relative transcription levels of IL-1β, IL-6, IL-8, IL-17, and TNF-α were quantified by RT-qPCR on day 8 post-challenge. β-actin was used as the internal reference gene, and the PBS Control group was used as the relative expression baseline. Data are presented as mean ± SEM. Different lowercase letters above the bars indicate significant differences between groups ($P < 0.05$); values sharing the same letter are not significantly different.

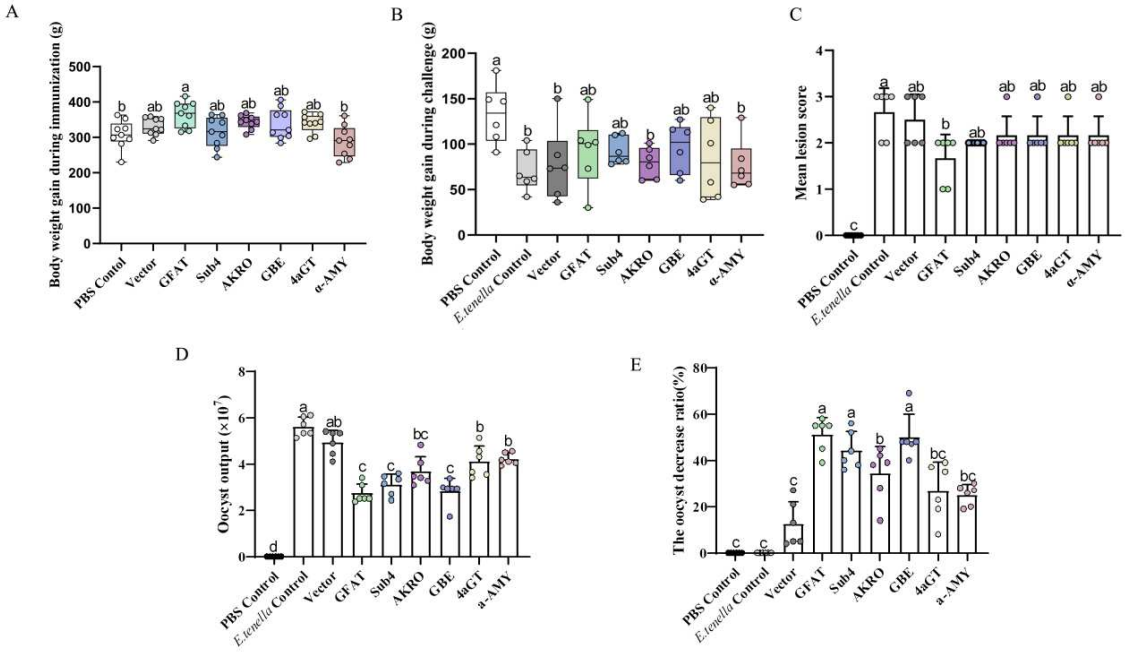

Fig. 9. Protective efficacy of the recombinant yeast vaccines in chickens challenged with *E. tenella*.

(A) Body weight gain during the immunization period. **(B)** Body weight gain during the challenge period. **(C)** Mean cecal lesion scores at day 8 post-challenge. **(D)** Total oocyst output per chicken from days 6 to 8 post-challenge. **(E)** Oocyst decrease ratio (%) of each immunized group relative to the *E. tenella* Control group. Data are presented as mean ± SEM. Different lowercase letters above the bars indicate significant differences between groups ($P < 0.05$).

Table 1. Primers used for gene amplification, plasmid construction, and sequencing.

Target Gene	Accession No.	Primer Name	Sequence (5'→3')*	Product Size (bp)
Glutamine-fructose-6-phosphate transaminase (*Et*GFAT)	ETH_00019125	pYD1-GFAT-F	*gtggtggtggttctgctagc*ACCATAATGAACAGAGACAAGCC	1200
		pYD1-GFAT-R	*taaaatgagccaccgccacc*CATACGCGCTAAAAGAGAGCC	
Subtilisin-like serine protease 4 (*Et*Sub4)	ETH_00006825	pYD1-Sub4-F	*gtggtggtggttctgctagc*GAAGTAGCTGCGGAGCCTCT	1200
		pYD1-Sub4-R	*taaaatgagccaccgccacc*GAACCCACG	

			ATTGCATACACACTT	
Aldo-keto reductase (*Et*AKRO)	ETH2_0912400	pYD1-AKRO-F	*gtggtggtggttctgctagc*ATGGGGGCCATCCAACCCGC	900
		pYD1-AKRO-R	*taaaatgagccaccgccacc*GGACTGAAGCAGAGGCATCTTGACACA	
1,4-alpha-glucan branching enzyme (*Et*GBE)	ETH_00033740	pYD1-GBE-F	*gtggtggtggttctgctagc*CCGTGGAACAAGTGGATTAT	498
		pYD1-GBE-R	*taaaatgagccaccgccacc*CTTGTATTCCTCAAGGAAAACAGC	
Alpha-1,4-galactosyltransferase (*Et*4aGT)	ETH2_0206400	pYD1-4aGT-F	*gtggtggtggttctgctagc*CATCCAACGTCGCTGCCTAG	1266
		pYD1-4aGT-R	*taaaatgagccaccgccacc*TTTTGTCTGTGGAGGAGACT	
Alpha-amylase (*Et*α-AMY)	ETH_00004695	pYD1-α-AMY-F	*gtggtggtggttctgctagc*CTGTGCTCCAAGCTGCAG	975
		pYD1-α-AMY-R	*taaaatgagccaccgccacc*GGTCCAAACACAGAAGTTAT	
Construct the pYD1-DCpep plasmid		DCpep-F	GGTGGCGGTGGCTCATTTTATCCATCATATCATTCAACTCCACAACGTCCAGAATTCTGCAGATATCCAGCACAGTG	382
		pYD1-DCpep-R	GCTAGCAGAACCACCACCAC	
Vector Backbone	-	pYD1-DCpep-F	GGTGGCGGTGGCTCATTTTA	-
		pYD1-DCpep-R	GCTAGCAGAACCACCACCAC	
AmpR Deletion	-	pYD1-KO-Amp-F1	CTGTCAGACCAAGTTTACTCATATATAC	-
		pYD1-KO-Amp-R1	GAGTCGTATTACAGCTGCTAGTA	
		pYD1-KO-Amp-F2	TACTAGCAGCTGTAATACGACTC	-
		pYD1-KO-Amp-R2	GTATATATGAGTAAACTTGGTCTGACAGCACATTTCCCCGAAAAGTGC	
Sequencing	-	pYD1-seq-F	AGTAACGTTTGTCAGTAATTGCGG	-
		pYD1-seq-R	CAAAGTCGATTTTGTTACATCTACACTG	

807 * Lowercase letters indicate the 20 bp homology arms complementary to the linearized pYD1

808 vector; uppercase letters indicate the gene-specific sequences.

809 **Table 2. Comprehensive evaluation of protection using the Anticoccidial Index (ACI)**

Group	Survival rate(%)	Relative weight gain rate(%)	Oocyst value	Cecal lesion value	ACI[1]	Protection level[2]
PBS Control	100	100	0	0	200	-
E.tenella Control	100	52	40	26	86	None
Vector	100	54	40	24	90	None
GFAT	100	71	10	18	143	Partial
Sub4	100	65	20	20	125	Partial
AKRO	100	60	20	22	118	None
GBE	100	70	10	22	138	Partial
4aGT	100	67	20	22	125	Partial
α-AMY	100	54	20	24	110	None

1 ACI was calculated as: (Survival Rate + Relative Weight Gain) – (OocystValue + Lesion Score).

2 Protection levels: Strong (>160), Partial (120–160), None (<120).

Supplementary Table S1. Primers used for quantitative real-time PCR.

Gene	Accession No.	Primer Name	Sequence (5'→3')	Product Size (bp)
β-actin (Beta-actin)	NM_205518.2	β-actin-F	GCCAACAGAGAGAAGATGACAC	140
		β-actin-R	GTAACACCATCACCAGAGTCCA	
IL-1β (Interleukin-1 beta)	NM_204524.2	IL-1β-F	GGTCAACATCGCCACCTACA	86
		IL-1β-R	CATACGAGATGGAAACCAGCAA	
IL-6 (Interleukin-6)	NM_204628.2	IL-6-F	ATGGTGATAAATCCCGATGAAG	153
		IL-6-R	CCTCACGGTCTTCTCCATAAAC	
IL-8 (Interleukin-8)	NM_205498.2	IL-8-F	AGTTCATCCACCCTAAATCC	233
		IL-8-R	CACACCTCTCTTCCATCCTT	
IL-17 (Interleukin-17)	NM_204460.2	IL-17-F	GAGAAGAGTGGTGGGAAAG	95
		IL-17-R	TCTACAAACTTGTTTATCAGCAT	
TNF-α (Tumor necrosis factor alpha)	NM_204267.2	TNF-α-F	GCCCTTCCTGTAACCAGATG	71
		TNF-α-R	ACACGACAGCCAAGTCAACG	
IL-2 (Interleukin-2)	NM_204153.2	IL-2-F	GTGGCTAACTAATCTGCTGTCC	105
		IL-2-R	GTAGGGCTTACAGAAAGGATCAA	
IL-4 (Interleukin-4)	NM_001007079.2	IL-4-F	CTGTGCCCACGCTGTGCTTA	83
		IL-4-R	GGAAACCTCTCCCTGGATGTCA	
IL-15 (Interleukin-15)	NM_204571.2	IL-15-F	TGCCAGGAACCTGTAATGAGATGT	100
		IL-15-R	TGTTCCGTACATCATGCTTCCTAC	

IFN-γ (Interferon gamma)	NM_205149.2	IFN-γ-F	CAAAGCCGCACATCAAACA	80
		IFN-γ-R	TTTCACCTTCACGCCATC	
IL-10 (Interleukin-10)	NM_001004414.4	IL-10-F	GGCTCACTTCCTCCTCC	94
		IL-10-R	TGACTTTCACCTGCAGATG	
Et-5S (Eimeria tenella 5S rRNA)	M86547	Et-5S-F	GCATCCCTCCATAACGCCACTTC	114
		Et-5S-R	CGTGTTGGTGTGCGTGTTTGTG	

813

814

Supplementary Files

This is a list of supplementary files associated with this preprint. Click to download.

- SupplementaryTableS1.doc